Effects of the Crystal Field on Transition Moments in 9-Ethylguanine†

David Theiste,‡,§ Patrik R. Callis,*,‡ and Robert W. Woody*,∥

Contribution from the Department of Chemistry, Montana State University, Bozeman, Montana 59717, and the Department of Biochemistry, Colorado State University, Fort Collins, Colorado 80523. *Received October 15, 1990*

Abstract: Molecular orbital calculations, both semiempirical and ab initio, give transition moment directions for purine and pyrimidine bases which frequently differ significantly from experimentally determined polarization directions. A particularly serious discrepancy exists in the case of 9-ethylguanine, in which the two lowest energy $\pi\pi^*$ transitions are predicted to have transition moment directions differing by 40–50° from the results of polarized reflection measurements on single crystals. The large ground-state dipole moments of the purine and pyrimidine bases lead to strong electrostatic interactions in the crystal which have been neglected in the MO calculations. The INDO/S Hamiltonian has been modified to include the effect of static charges in the environment of the molecule. The resulting modifications in the Fock matrix require the calculation of the electrostatic potential and field at each atomic center. These have been evaluated for 9-methylguanine as a model for 9-ethylguanine by using the known crystal structure of the latter. Ground-state charges calculated in the Mulliken approximation were evaluated from INDO/S wave functions, and the potentials and fields included contributions from all molecules in four unit cells in each direction from the central molecule. Polarization effects were included by an iterative procedure in which the initial charges, calculated for an isolated molecule, were replaced by those calculated for the molecule in the crystal field. This process was repeated until the resulting transition moment directions differed by less than 0.1° between successive cycles. Additional calculations were performed with charges which had been scaled down so that the dipole moment calculated for the isolated molecule agrees with that estimated from ab initio calculations. The results of these calculations show marked improvement in agreement with experiment. The residual discrepancy for the first $\pi\pi^*$ transition is 6–18° and that for the second is 24–29°, where the smaller value is from unscaled calculations and the larger from scaled. Comparison with data for higher energy transitions also shows greatly improved agreement with experiment, especially for the scaled calculations. The results also indicate substantial mixing of $n\pi^*$ and $\pi\pi^*$ excited states by the crystal field, which could be significant for the circular dichroism of nucleic acids. We conclude that local electrostatic fields in crystals can substantially modify the excited states and transition parameters of the bases of nucleic acids. Clearly these effects must be considered in theoretical treatments of the optical properties of DNA and RNA.

To understand the optical properties of DNA and RNA, we need to know the transition dipole moments of the component bases. Experimental and theoretical efforts to provide these data have been reviewed.[1] The most direct experimental method of determining transition moment directions is polarized absorption or reflection spectroscopy of single crystals. However, polarized absorption and reflection spectroscopy generally give two alternative directions for the transition moment.

Figure 1 shows a comparison of the experimental transition moment directions[2] for the first two $\pi\pi^*$ transitions in 9-ethylguanine with the directions calculated by various semiempirical MO methods. There are discrepancies of at least 40° for the first and second transitions in nearly all of these calculations. One calculation (panel I) gives a transition moment direction for the first $\pi\pi^*$ transition that is within less than 20° of the experimental value, but the second transition is still more than 40° off. Moreover, the far-UV transitions are poorly reproduced in all extant calculations. Interestingly, the semiempirical calculations, regardless of whether only π-electrons are considered or all valence electrons are included, and despite variations in parametrization, show a strong consensus for the first $\pi\pi^*$ transition to be polarized at −50° to −70° (in the DeVoe–Tinoco[12] convention) and the second transition at 40–60°. Ab initio calculations[13] have yielded results that are in general agreement with the semiempirical MO calculations and not with experiment.

A possible reason for this discrepancy is that the MO calculations refer to the isolated molecule, while the experimental results are for the molecule in a crystal, subject to interactions with neighboring molecules. Two such types of interaction have long been considered in analyses of molecular crystal spectra. Resonance coupling occurs between identical transitions on different molecules, leading to Davydov[14] splitting of the zeroth-order degenerate levels. Transition moments for different transitions on neighboring molecules also interact, leading to mixing of excited states and reorientation of the transition moments. These effects have been carefully analyzed in the crystal spectra of several purines.[15,16] The spectra of 9-ethylguanine were not subjected to such an analysis[2] because of the complex crystal structure (2 molecules per asymmetric unit and 16 molecules per unit cell[17]) and because only one well-developed crystal face was available for study. However, on the basis of previous experience, Clark[2] estimated that these effects should introduce no more than ca. 10° deviations from the oriented gas model.

Another type of intermolecular interaction, with the local electrostatic field, may be of greater significance in highly polar crystals such as those of the purine and pyrimidine bases. In a strong electric field, changes in the permanent dipole upon excitation can lead to significant shifts in excited-state energy, possibly leading to reversals in the order of excited states relative

† Dedicated to Professor Ignacio Tinoco, Jr., on the occasion of his 60th birthday.

‡ Montana State University.
§ Present address: Gentex Corp., 600 N. Centennial, Zeeland, MI 49464.
∥ Colorado State University.

(1) Callis, P. R. *Annu. Rev. Phys. Chem.* **1983**, *34*, 329.
(2) Clark, L. B. *J. Am. Chem. Soc.* **1977**, *99*, 3934.
(3) Del Bene, J.; Jaffe, H. H. *J. Chem. Phys.* **1968**, *48*, 1807.
(4) Srivastava, S. K.; Mishra, P. C. *Int. J. Quantum Chem.* **1979**, *16*, 1051.
(5) Hug, W.; Tinoco, I., Jr. *J. Am. Chem. Soc.* **1973**, *95*, 2803.
(6) Ito, H.; I'Haya, Y. J. *Bull. Chem. Soc. Jpn.* **1976**, *49*, 3466.
(7) Danilov, V. I.; Pechenya, V. I.; Zheltovsky, N. V. *Int. J. Quantum Chem.* **1980**, *17*, 307.
(8) Ridley, J.; Zerner, M. *Theor. Chim. Acta* **1973**, *32*, 111.
(9) Callis, P. R. *Photochem. Photobiol.* **1986**, *44*, 315.
(10) Karlsson, G.; Maortesson, O. *Theor. Chim. Acta* **1969**, *13*, 195.
(11) Srivastava, S. K.; Mishra, P. C. *Int. J. Quantum Chem.* **1980**, *18*, 827.
(12) DeVoe, H.; Tinoco, I., Jr. *J. Mol. Biol.* **1962**, *4*, 500.
(13) Petke, J. D.; Maggiora, G. M.; Christoffersen, R. E. *J. Am. Chem. Soc.* **1990**, *112*, 5452.
(14) Davydov, A. S. *Theory of Molecular Excitons*; Dresler, S. B., Translator; Plenum Press: New York, 1971.
(15) Chen, H. H.; Clark, L. B. *J. Chem. Phys.* **1969**, *51*, 1962.
(16) Chen, H. H.; Clark, L. B. *J. Chem. Phys.* **1973**, *58*, 2593.
(17) Destro, R.; Kistenmacher, T. J.; Marsh, R. E. *Acta Crystallogr.* **1974**, *B30*, 79.

0002-7863/91/1513-3260$02.50/0

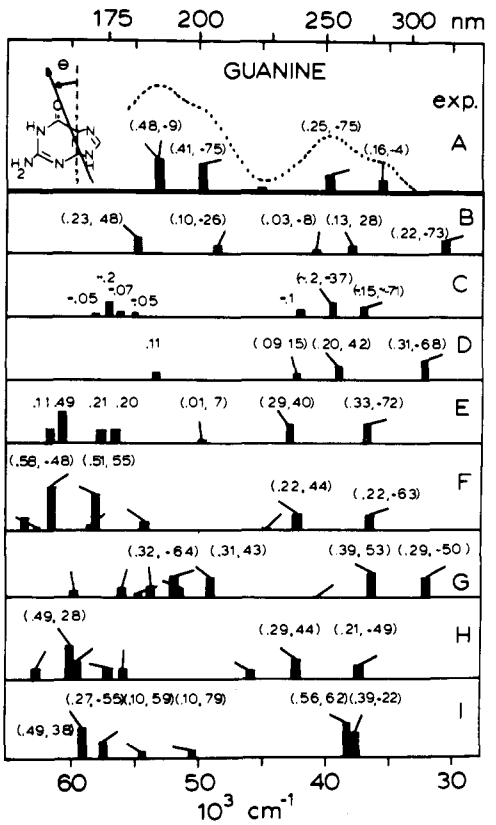

Figure 1. Comparison of experimental transition parameters for 9-ethylguanine crystals with theoretical values obtained for guanine. (A) Experimental data of Clark;[2] (B) CNDO/S[3] calculations of Srivastava and Mishra;[4] (C) CNDO calculations of Hug and Tinoco;[5] (D) CNDO/S with renormalized self-consistent random phase approximation;[6] (E) CNDO/S calculations of Danilov et al.;[7] (F) INDO/S[8] calculations of Callis,[9] using singly and doubly excited configurations; (G) INDO/S[8] calculations (singly excited configurations only) of Callis;[9] (H) calculations of Callis[9] simulating the Hug and Tinoco[5] CNDO parameterization; (I) variable-electronegativity PPP[10] calculations of Srivastava and Mishra.[11] The arrows represent the transition moment directions, and the heights of the solid bars give the relative oscillator strength. Numerical values in parentheses give the oscillator strength first, followed by the transition moment direction, specified in the DeVoe–Tinoco[12] convention, defined in the upper left.

to the gas phase. In addition, the local electrostatic field can mix the excited states, leading to changes in transition moment direction. Although these effects have been anticipated and discussed, the lack of data on excited-state charge distributions and transition charge densities connecting excited states has prevented their incorporation in analyses of crystal spectra.

Noting the large ground-state dipole moment[18-20] of guanine and the large changes in dipole moment upon excitation,[21] Woody[22] suggested that electrostatic effects in 9-ethylguanine crystals are largely responsible for the discrepancy between theory and experiment. The excited states predicted by MO theory were used as a basis set, and perturbation theory was applied to calculate the excited-state mixing and energy-level shifts produced by electrostatic interactions in 9-ethylguanine crystals. The results were encouraging in that the discrepancies between theory and experiment were decreased by roughly a factor of 2 for the first two excited states of 9-ethylguanine.

In the present study, crystal field effects on the electronic structure of 9-ethylguanine are treated by a different method. The time-average field of the surrounding molecules is included in the Hamiltonian, leading to a modified Fock matrix. The resulting self-consistent field equations are then solved in the usual way, followed by configuration interaction. The resulting transition moment directions are in better agreement with experiment than those obtained by diagonalizing the electrostatic perturbation matrix using gas-phase excited states as a basis.[22]

Theory

The molecule of interest experiences an electrostatic field created by a set of point charges, q_α, located at points $\mathbf{R}_\alpha$. The Fock operator is therefore modified as follows[23]

$$\hat{F} = \hat{F}_0 - e\sum_\alpha q_\alpha / R_{i\alpha} \tag{1}$$

where $\hat{F}_0$ is the Fock operator for the free molecule and $R_{i\alpha}$ is the distance from the ith electron to the point charge α.

Consider an electron in an orbital centered on atom a at position $\mathbf{R}_a$. The position of the electron can then be written as

$$\mathbf{R}_i = \mathbf{R}_a + \mathbf{r}_{ai} \tag{2}$$

where $\mathbf{r}_{ai}$ is the position of electron i relative to nucleus a. Then

$$R_{i\alpha} = |\mathbf{R}_\alpha - \mathbf{R}_i| = |\mathbf{R}_\alpha - \mathbf{R}_a - \mathbf{r}_{ai}| \tag{3}$$

In general,

$$R_{a\alpha} = |\mathbf{R}_\alpha - \mathbf{R}_a| \gg |\mathbf{r}_{ai}| \tag{4}$$

so we can expand the summation in eq 1:

$$-e\sum_\alpha \frac{q_\alpha}{R_{i\alpha}} = -e\sum_\alpha \frac{q_\alpha}{R_{a\alpha}} - e\sum_\alpha \frac{q_\alpha \mathbf{R}_{a\alpha}\cdot\mathbf{r}_{ai}}{R_{a\alpha}^3} + \sum_\alpha \mathcal{O}(r_{ai}^2/R_{a\alpha}^3) \tag{5}$$

$$-e\sum_\alpha \frac{q_\alpha}{R_{i\alpha}} = -eV_a + e\mathbf{E}_a\cdot\mathbf{r}_{ai} - e\mathcal{O}(\mathbf{r}_{ai}\cdot\mathbf{Q}_a\cdot\mathbf{r}_{ai}) \tag{6}$$

Here, V_a is the potential at nucleus a due to the set of point charges, $\mathbf{E}_a$ is the electrostatic field at nucleus a, and $\mathbf{Q}_a$ is the quadrupole tensor.

We now consider matrix elements of these operators over the atomic orbitals ϕ_μ and ϕ_ν. First, by the zero-differential overlap approximation, the matrix elements will vanish unless ϕ_μ and ϕ_ν are located on the same atom, a. For diagonal elements of the Fock matrix, we have

$$F_{\mu\mu} = F^\circ{}_{\mu\mu} - eV_a \tag{7}$$

where we have neglected the second order and higher order terms in eq 6. For off-diagonal elements between ϕ_μ and ϕ_ν, both located on atom a, the contribution of the leading term in eq 6 vanishes, so we have

$$F_{\mu\nu} = F^\circ{}_{\mu\nu} + e\mathbf{E}_a\cdot\mathbf{r}_{\mu\nu} \tag{8}$$

For the type of systems of interest here, $\mathbf{r}_{\mu\nu}$ is zero unless μ is a 2s orbital and ν a 2p orbital or vice versa. For example, if ν = 2s, ν = $2p_x$, we have

$$\mathbf{r}_{2s,2p_x} = \frac{5}{2\sqrt{3}\zeta_a}\mathbf{i} \tag{9}$$

where ζ_a is the orbital exponent for atom a.

Thus, we need to calculate the electrostatic potential and the electric field at each atomic center due to the neighboring molecules in the crystal. These potentials and fields are included in the Fock matrix elements in the SCF process.

The electrostatic potentials and electric fields are calculated by using ground-state wave functions for the isolated molecule. The neighboring molecules make two kinds of contributions to the electrostatic potentials and fields at the molecule of interest. Each atomic center of a ground-state molecule will carry a net charge given by

$$q_A = -e(\sum_\beta P_{\beta\beta} - Z_A) \tag{10}$$

(18) Pullman, B.; Pullman, A. *Prog. Nucleic Acid Res. Mol. Biol.* **1969**, *9*, 327.
(19) Clementi, F.; Andre, J. M.; Andre, M. C.; Klint, D.; Hahn, D. *Acta Phys. Chem.* **1969**, *27*, 493.
(20) Singh, U. C.; Kollman, P. A. *J. Comput. Chem.* **1984**, *5*, 129.
(21) Srivastava, S. K.; Mishra, P. C. *J. Mol. Struct.* **1980**, *65*, 199.
(22) Woody, R. W. *Biophys. J.* **1984**, *45*, 232a.
(23) Honig, B.; Greenberg, A. D.; Dinur, U.; Ebrey, T. G. *Biochemistry* **1976**, *15*, 4593.

where $P_{\beta\beta}$ is the diagonal element of the bond order–charge density matrix for orbital β centered on atom A. The summation over all orbitals on the atom gives the number of electrons assignable to atom A, while Z_A is the charge of the atomic core.

Atoms other than H will also have dipoles resulting from sp mixing, which causes the center of gravity of the electron density to be displaced from the nucleus. This contribution, sometimes referred to as a hybridization moment, is particularly pronounced for atoms with lone pairs, such as the keto oxygen and the pyridine-type ring nitrogens, N_3 and N_7, of 9-ethylguanine. These dipolar charge distributions can be approximated by two point charges

$$q_{sp_x} = \pm\sqrt{3}eP_{sp_x}/4 \tag{11}$$

located at $\pm(5/3\zeta)$i from the nucleus along the x axis and similarly along the y and z axes. P_{sp_x} is the off-diagonal element of the bond order matrix connecting the 2s and the $2p_x$ orbitals of the atom in question. (In the absence of σ–π mixing, there will be no such dipoles in the z direction, but since the crystal field breaks the symmetry plane of the molecule, there will be a z component of the dipole in the crystal.)

There are two alternative ways[24] of deriving atomic charge densities and sp monopoles from wave functions derived by a ZDO method such as INDO/S.[8] The simplest one uses the charge density–bond order matrix elements obtained in the SCF process. Such atomic and sp monopole changes are said to be in the Löwdin basis.[25] However, Löwdin orbitals are not strictly localized on individual atomic centers but are orthogonalized linear combinations of Slater atomic orbitals. The Mulliken[26] population analysis uses deorthogonalized orbitals, i.e., a Slater basis. Shillady et al.[27] have provided evidence that the Mulliken populations give better predictions of dipole moments. In the present paper, only results obtained with the Slater basis will be reported.

Methods

The structure of the 9-methylguanine molecule was derived from the crystal structure[17] of 9-ethylguanine. The methyl derivative was used as a model of 9-ethylguanine to simplify the calculations. Both molecules A and B of the asymmetric unit were idealized by imposing a plane of symmetry. The crystal coordinates for molecules A and B were transformed into a right-handed Cartesian coordinate system in which the z axis was taken to be the normal to the best plane through the nine atoms of the purine ring. The y axis was taken to be mutually perpendicular to the z axis and the C_4–C_5 direction and the x axis to be orthogonal to both y and z axes. After transformation to this coordinate system, the largest deviation of the nine purine ring atoms from the xy plane was 0.024 Å (in molecule A), and the rms deviations were 0.015 Å for molecule A and 0.009 Å for molecule B. Of the other atoms, other than protons on the 9-methyl group, the 2-amino hydrogens were furthest out of the plane, 0.22 and 0.28 Å for molecule A and 0.02 and 0.22 Å for molecule B. The z coordinate of all atoms other than the 9-methyl protons was set equal to zero. The 9-methyl group was taken to be tetrahedral and the rotamer with one proton in plane and cis to C_8 was chosen, with the other two protons symmetrically disposed with respect to the xy plane. The coordinates are given in Table I.

The INDO/S[8] calculations were performed on 9-methylguanine assuming these idealized geometries. The results for molecules A and B showed small differences in both ground- and excited-state properties. For calculations of the electrostatic potential and field, a molecule with this idealized A geometry was placed at A lattice sites, while B lattice sites were occupied by idealized B molecules. The centers of the idealized molecules, the midpoint of the C_4–C_5 bond, were superimposed on the corresponding points in the crystal structure. Appropriate transformation matrices were used to correctly orient the idealized molecules at the A and B sites.

The spectroscopically calibrated semiempirical MO method used in this study is a version of INDO/S kindly provided by Professor Michael Zerner,[8] University of Florida, in 1984. We have used this program extensively.[9,28] For this work 196 singly excited configurations were used in the configuration interaction, arising from excitations from the 14 highest filled to the 14 lowest unoccupied MOs. Accordingly, the Mataga–Nishimoto[29,30] electron–electron repulsion integral parameters were chosen. The p_σ and p_π overlap weighting factors were 1.267 and 0.585, respectively. Results for relative state energies, intensities, and polarizations were insensitive to changes in the number of configurations and whether doubly excited configurations were used.

Charges were calculated for each atomic center in the deorthogonalized basis.[26,27] For calculations of the electrostatic potential and fields at a central molecule, these charges were located at the nuclei of the surrounding molecules. Point charges corresponding to the hybridization or sp dipoles were also calculated from the deorthogonalized wave functions and were placed at distances of $\pm 5a_0/(3\zeta)$ from the nucleus along the x, y, and z directions of the molecular coordinate system.

The electrostatic potential and the electric field at a given nucleus a in the central molecule were calculated from the expressions

$$V_a = \sum_i \sum_j \frac{q_{ij}}{R_{ij_a}} \tag{12}$$

$$\mathbf{E}_a = \sum_i \sum_j \frac{q_{ij}}{R_{ij_a}^3} \mathbf{R}_{ij_a} \tag{13}$$

where q_{ij} denotes the jth charge on molecule i, $\mathbf{R}_{ij_a} = \mathbf{R}_a - \mathbf{R}_{ij}$ is the vector from the charge ij to the nucleus a, and R_{ij_a} is the magnitude of this vector. The summations are over all charges and, in principle, all molecules. In practice, the summation extended over four unit cells in the $\pm a$, $\pm b$, and $\pm c$ directions, as well as the unit cell containing the central

Table I. Idealized Molecular Geometries of 9-Methylguanine[a]

	molecule A			molecule B		
atom	x	y	z	x	y	z
N1	0.502	2.307	0	0.490	2.311	0
C2	−0.870	2.204	0	−0.871	2.204	0
N3	−1.522	1.057	0	−1.531	1.060	0
C4	−0.687	0.003	0	−0.690	−0.001	0
C5	0.693	0.003	0	0.684	−0.001	0
C6	1.379	1.225	0	1.372	1.231	0
N7	1.169	−1.292	0	1.183	−1.296	0
C8	0.096	−2.042	0	0.108	−2.054	0
N9	−1.060	−1.318	0	−1.059	−1.328	0
N10	−1.563	3.349	0	−1.553	3.364	0
O11	2.601	1.427	0	2.592	1.434	0
H1	0.889	3.135	0	0.907	3.201	0
H2	−1.176	4.244	0	−1.120	4.250	0
H2′	−2.419	3.265	0	−2.474	3.230	0
H8	0.146	−3.005	0	0.077	−3.101	0
C9	−2.442	−1.832	0	−2.440	−1.839	0
H9	−2.448	−2.921	0	−2.446	−2.929	0
H9′	−2.954	−1.466	0.890	−2.952	−1.474	0.890
H9″	−2.954	−1.466	−0.890	−2.952	−1.474	−0.890

[a] The coordinate axes and numbering system are shown below.

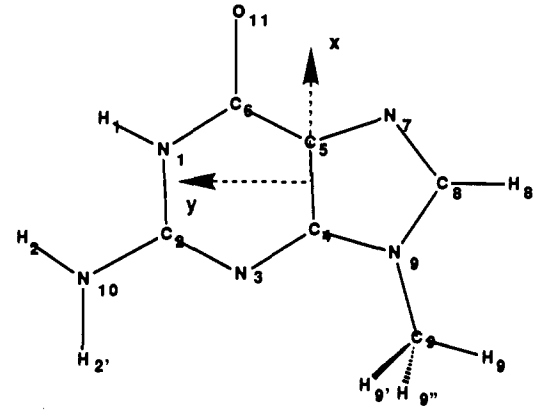

Coordinates are in angstroms.

(24) Sadlej, J. *Semi-Empirical Methods of Quantum Chemistry*; Ellis Horwood: Chichester, England, 1985; pp 142–160.
(25) Löwdin, P. O. *J. Chem. Phys.* **1950**, *18*, 365.
(26) Mulliken, R. S. *J. Chem. Phys.* **1955**, *23*, 1833.
(27) Shillady, D. D.; Billingsley, F. P.; Bloor, J. E. *Theor. Chim. Acta* **1971**, *21*, 1.
(28) Eftink, M. R.; Selvidge, L. A.; Callis, P. R.; Rehms, A. R. *J. Phys. Chem.* **1990**, *94*, 3469.
(29) Mataga, N.; Nishimoto, K. *Z. Phys. Chem. (Frankfurt/Main)* **1957**, *12*, 335.
(30) Mataga, N.; Nishimoto, K. *Z. Phys. Chem. (Frankfurt/Main)* **1957**, *13*, 140.

Table II. Ground-State Dipole Moment

	iteration[a]	$\|\mu\|$[b]	θ[c]
	Molecule A		
gas phase	0U	10.16	165.6
crystal	1U	12.30	157.1
	5U	13.14	156.6
gas phase	0S	8.23	165.6
crystal	1S	9.61	158.5
	5S	10.02	158.1
	Molecule B		
gas phase	0U	9.99	165.8
crystal	1U	12.94	158.7
	5U	13.77	158.7
gas phase	0S	8.09	165.8
	1S	10.00	159.8
	5S	10.41	159.8
gas phase[d]		6.24	151.6
gas phase[e]		6.59	155.3

[a] The zeroth iteration is for the isolated molecule. Iteration 1 is for the crystal, using charges calculated for the isolated molecule. Iteration 5 is the final calculation. S indicates that a scaling factor (0.81) was applied (see text), while U indicates an unscaled calculation. [b] Dipole moment magnitude, in Debyes (10^{-18} esu cm). [c] Direction of dipole moment, specified in the convention of DeVoe and Tinoco.[12] [d] Ab initio (STO-3G) results of Singh and Kollman[20] using an STO-3G basis set. [e] Ab initio results of Singh and Kollman[20] using the minimal basis set of Clementi et al.[19]

molecule. Thus, a total of 11 663 surrounding molecules were included.

To take polarization into account, the calculation was iterated to self-consistency. The charges calculated for the ground-state wave function obtained by using electrostatic potentials and electric fields derived from isolated molecule charges were used to generate a new set of potentials and fields. These were then incorporated in the INDO/S calculation to obtain a new set of ground-state charges, and the process was repeated until successive calculations gave transition moment directions that agreed with 0.1°.

Two sets of charges were used in the calculations. The first set was derived from the INDO/S wave functions, as just described. For the second set, these charges were scaled down by a factor of 0.81. The justification for this scaling factor is as follows. Ideally, a scaling factor would be calculated from the ratio of the observed ground-state dipole moment of 9-methylguanine to that calculated by INDO/S. However, there are no experimental dipole moment data available for 9-methylguanine or other guanine derivatives. Ab initio estimates of the dipole moment of 9-methylguanine have been reported[20] (Table II), but the minimal basis sets used may not give a very accurate dipole moment. Williams and Yan[31] have recommended that STO-3G dipole moments be scaled up by a factor of 1.27. Applying this factor to the average of the values reported by Singh and Kollman[20] (6.42 D), we have an estimate for the experimental value of 8.15 D. Comparison of this value with the 10.1 D obtained for the isolated molecule from INDO/S calculations gives a scale factor of 0.81. In our scaled calculations, this factor was applied to the net atomic charges and to the sp monopoles. It was assumed that the same factor is applicable to successive iterations.

For comparison of theoretical results with experiment, it is necessary to average the transition parameters for molecules A and B and, in some cases, to combine two or more transitions on each molecule. The wavelengths were averaged after each contributing transition was weighted by its dipole strength (μ^2), although a simple averaging process gave essentially the same results. The oscillator strength of the combined transitions was calculated from the total dipole strength and the averaged wavelength

$$\langle f \rangle = 2.3513 \sum_i \mu_i^2 / \langle \lambda \rangle \qquad (14)$$

where the summation is over the component transitions, $\langle \lambda \rangle$ is the average wavelength in nanometers, and the units of the dipole strength are Debye.[2] A factor of $^1/_2$ has been included in eq 14 to obtain the average per molecule. The theoretical average transition moment directions were obtained by transforming each component transition moment into the crystal coordinate system and then calculating the dichroic ratio I_c/I_{ab} by summing the contributions along the appropriate crystal axes. The two possible in-plane transition moment directions consistent with this calculated dichroic ratio were calculated for molecules A and B, and the angles for the two molecules were averaged.

(31) Williams, D. E.; Yan, J.-M. *Adv. At. Mol. Phys.* **1988**, *23*, 87.

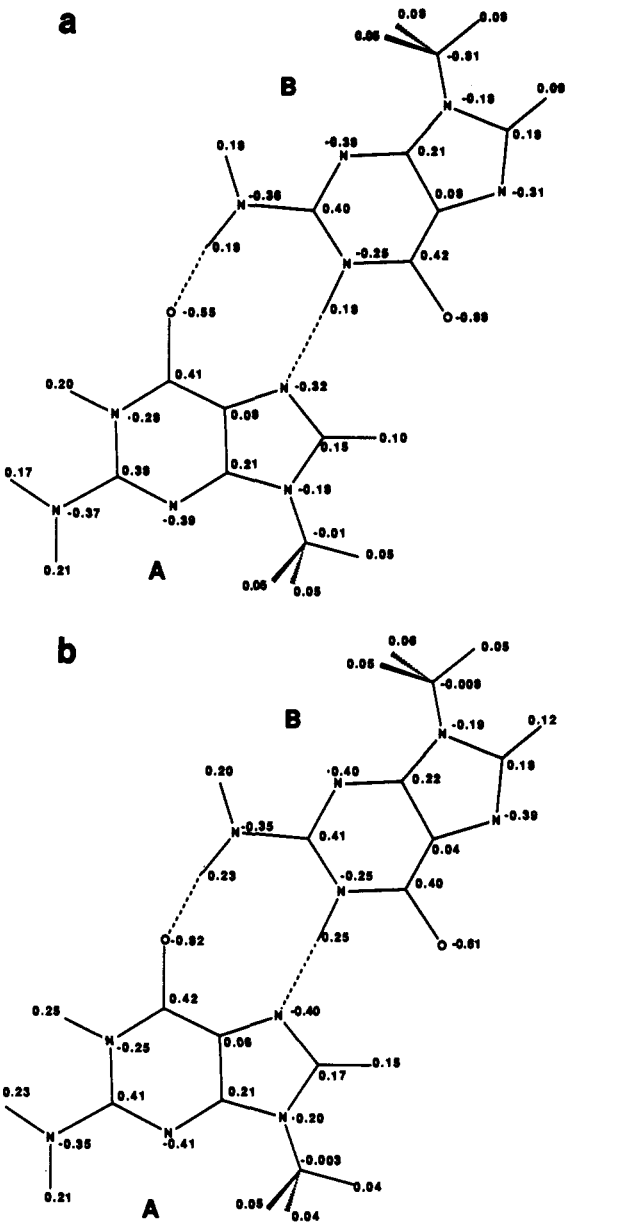

Figure 2. Net atomic charges calculated for molecules A and B by using deorthogonalized wave functions, in atomic units (a) for the isolated molecules and (b) for the molecules in the crystal after convergence was attained. A scaling factor of 0.81 was used for both sets of charges.

Results

Figure 2 shows the net atomic charges calculated for the isolated A and B molecules and those calculated in the final iterations, using the scaling factor. Polarization effects in the crystal cause the charges of atoms involved in hydrogen bonding to have a larger net charge than they have in the isolated molecules. The H-bond acceptor atoms, N_7 and O_{11}, have net charges about 10% larger, while the increases for the protons involved in H bonding, H1 and H2, are larger by ca. 20%. Atoms not directly involved in the H bonds, even N_1 and N_{10}, show little difference in charge.

In Figure 3, the local dipole moments arising from the sp monopoles at each first-row atoms are shown. These local dipole moments are large for N_3, N_7, and O_{11} (ca. 2.4, 2.3, and 1.3 D, respectively) and small for the other atoms. The crystal environment has little effect on these local dipole moments, with the three major dipoles changing by less than 1% from the gas phase to the final iteration in the crystal.

Table II shows the dipole moments for molecules A and B in the gas phase and in the crystal. The crystal results are reported for the first iteration using charges calculated for the isolated molecule and for the final iteration. The results are compared

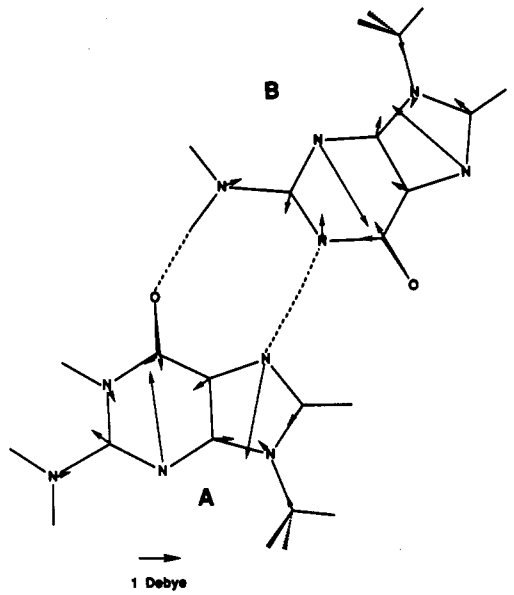

Figure 3. Hybridization dipole moments centered at each second row atom. The dipoles shown are for the isolated molecules, but these do not change significantly upon application of the crystal field.

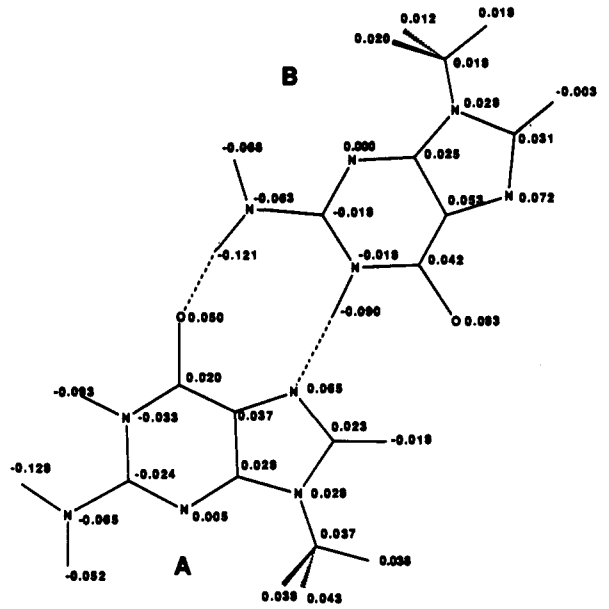

Figure 4. Calculated potentials at the atomic centers in the final iteration using scaled charges, in atomic units (e/a_0 = 9.0768 × 10^{-2} statcoulomb/cm).

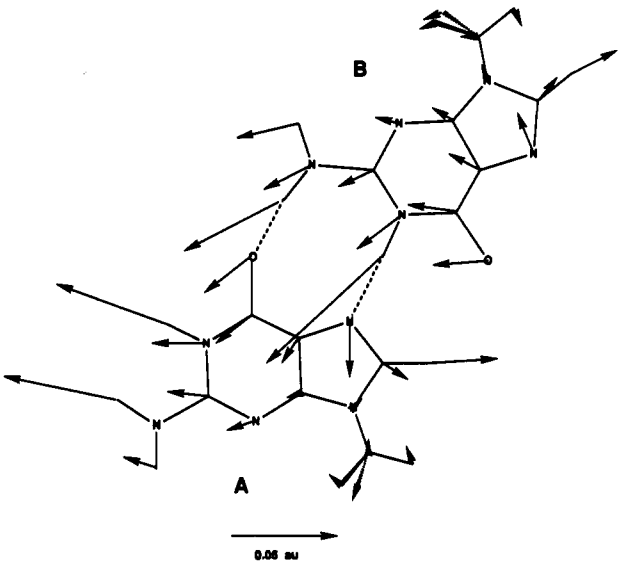

Figure 5. Electrostatic field at the atomic centers in the final iteration using scaled charges, in atomic units (e/a_0^2 = 1.7153 × 10^7 statcoulomb/cm^2).

with ab initio calculations[20] using an STO-3G basis set and another minimal basis set.[19] The differences between molecules A and B for the isolated molecule are very small, stemming from slight differences in molecular geometry. Larger differences are predicted in the crystal (ca. 4–5% in magnitude, 2° in direction), reflecting the somewhat different environment of the two molecules in the asymmetric unit. The crystal environment increases the dipole moment by about 20% in the scaled calculations and by ca. 30% in the unscaled results, with respect to the dipole moment of the isolated molecule. The direction is also affected, rotating through −9°. Comparison with the ab initio result has been previously mentioned in connection with the choice of the scaling factor. It should be noted that use of a scaling factor implies that the directions of the dipole moments are the same. This is not strictly correct, as the gas-phase INDO/S dipole moments differ by about 14° from the STO-3G ab initio direction, and it is not known which is closer to the true dipole moment direction.

The potentials at each of the atoms in the final iteration (scaled) are shown in Figure 4. The potentials have been adjusted by the addition of a constant so that the average over the atoms is zero. As expected, the atoms with the most negative potentials are hydrogens H_1 and H_2 which participate in hydrogen bonds, while those atoms with the most positive potentials are O_{11} and N_7, which act as H-bond acceptors. The overall range of potentials is ca. 0.2 au (5.3 eV) when a scaling factor is used and 0.25 au (6.8 eV) when unscaled charges are used. The net atomic charges make the largest contribution to the potentials, generally 2–3 times larger than the sp monopoles, consistent with the relative contributions to the calculated ground-state dipole moment. Nevertheless, the sp monopoles contribute to a significant extent.

Figure 5 shows the electrostatic field at each center, again for the scaled calculation. The strongest fields are experienced by atoms involved in H bonding, with protons H_1 and H_2 subjected to the strongest fields, which are oriented toward the H-bond acceptors. The fields at the H-bond acceptors, N_7 and O_{11}, are somewhat smaller and oriented away from the H-bond donors. The sp monopoles generally contribute less to the electric field at the various centers by a factor of 2–3, but in the case of H_1, the sp monopole contribution is stronger than that of the net atomic charges.

Tables III and IV give the predicted transition parameters for the $\pi\pi^*$ and $n\pi^*$ transitions, comparing the results for the isolated molecule with those for calculations including both scaled and unscaled crystal fields. The $\pi\pi^*$ transition parameters using scaled charges are compared graphically with experiment in Figure 6. In the absence of the field, the molecular plane of symmetry assures that $n\pi^*$ and $\pi\pi^*$ transitions are distinct. Since the crystal field breaks this symmetry, the two types are not distinct in the calculations incorporating the field. An arbitrary distinction has been drawn in constructing Tables III and IV. Transitions with transition moments less than 10° out-of-plane are considered as $\pi\pi^*$ transitions and are included in Table III, while all others are considered as $n\pi^*$ transitions.

Discussion

The most striking effect of the crystal field is the change in transition moment directions for the first two $\pi\pi^*$ transitions. In the scaled calculations, the transition moment for the first $\pi\pi^*$ transition undergoes rotations of +22° and +31° in molecules A and B, respectively, and the second transition has its polarization altered by +17° and +21°, respectively. The unscaled calculations lead to significantly larger rotations, by 8° for the first transition and by 5° for the second transition. The field on molecule B leads to larger changes in transition moment direction for both transitions.

The first two $\pi\pi^*$ transitions are predicted to undergo small changes in energy and intensity due to the crystal field. The

Table III. Predicted $\pi\pi^*$ Transitions

gas phase			crystal (scaled)			crystal (unscaled)		
λ	*f*	θ	λ	*f*	θ	λ	*f*	θ
			Molecule A					
315	0.28	−44	309	0.25	−22	310	0.23	−14
275	0.38	57	277	0.42	74	283	0.04	83
242	0.01	−44	241	0.07	79	280	0.35	79
210	0.47	56	204	0.33	−21	239	0.12	84
201	0.19	−63	202	0.41	−90	207	0.45	−34
194	0.10	−22	197	0.06	13	202	0.11	61
190	0.10	30	195	0.03	−4	200	0.21	84
182	0.15	−43	193	0.06	−40	196	0.07	5
179	0.18	−16	185	0.29	17	193	0.05	−41
171	0.17	10	177	0.05	−25	185	0.26	19
161	0.08	−74	170	0.04	5	175	0.02	−25
			169	0.00	44	174	0.00	24
			163	0.06	40	172	0.03	15
						169	0.00	47
						166	0.06	6
						162	0.09	56
			Molecule B					
311	0.28	−45	310	0.24	−14	314	0.22	−6
275	0.38	57	277	0.42	78	280	0.39	83
243	0.01	−34	240	0.08	80	240	0.13	88
210	0.46	55	208	0.47	−62	211	0.54	−50
202	0.19	−60	204	0.23	30	207	0.14	42
193	0.10	−24	199	0.06	−41	203	0.08	56
190	0.10	33	194	0.00	12	194	0.02	−5
183	0.14	−44	192	0.04	−41	193	0.05	−33
180	0.20	−14	188	0.32	16	188	0.29	17
172	0.16	10	179	0.06	−27	178	0.08	6
162	0.08	−73	174	0.06	17	177	0.02	73
			164	0.06	59	166	0.02	−50
			163	0.01	66	165	0.09	43
						164	0.04	53

Table IV. Predicted $n\pi^*$ Transitions

gas phase			crystal (scaled)			crystal (unscaled)		
λ	10^2f	ϕ^a	λ	10^2f	ϕ^a	λ	10^2f	ϕ^a
			Molecule A					
326	0.12	90	293	0.17	44	230	0.07	44
244	0.02	90	228	0.04	55	222	1.02	37
240	2.50	90	222	0.10	31	216	0.28	79
218	0.09	90	220	0.55	66	209	2.95	81
217	1.17	90	214	3.15	87	181	0.37	70
205	0.29	90	186	0.51	54	172	0.75	39
195	0.16	90	175	0.25	74	164	0.54	75
187	0.82	90	171	0.37	72			
173	0.27	90	164	0.69	68			
167	0.00	90	160	0.54	35			
166	1.16	90						
164	0.51	90						
162	0.08	90						
			Molecule B					
325	0.11	90	294	0.10	60	284	0.23	32
241	0.17	90	230	0.09	17	235	0.23	30
236	2.60	90	223	0.06	69	223	0.75	65
218	0.64	90	220	0.55	65	219	0.09	42
215	0.54	90	215	3.55	88	212	4.06	63
204	0.32	90	182	0.30	80	176	0.53	45
197	0.04	90	176	0.38	55	174	0.19	38
188	1.07	90	168	0.06	26	167	0.29	14
170	0.25	90	165	1.53	45	165	0.68	76
168	0.00	90	163	0.86	83	163	0.89	86
167	1.67	90						
164	0.50	90						
161	0.02	90						
160	1.00	90						

[a] ϕ is the angle that the transition dipole makes with respect to the molecular plane.

wavelength shifts are predicted to be only a few nanometers and are of doubtful significance. In both molecules, the first band is slightly weaker in the presence of the crystal field and the second band becomes slightly stronger. (This latter trend is obscured

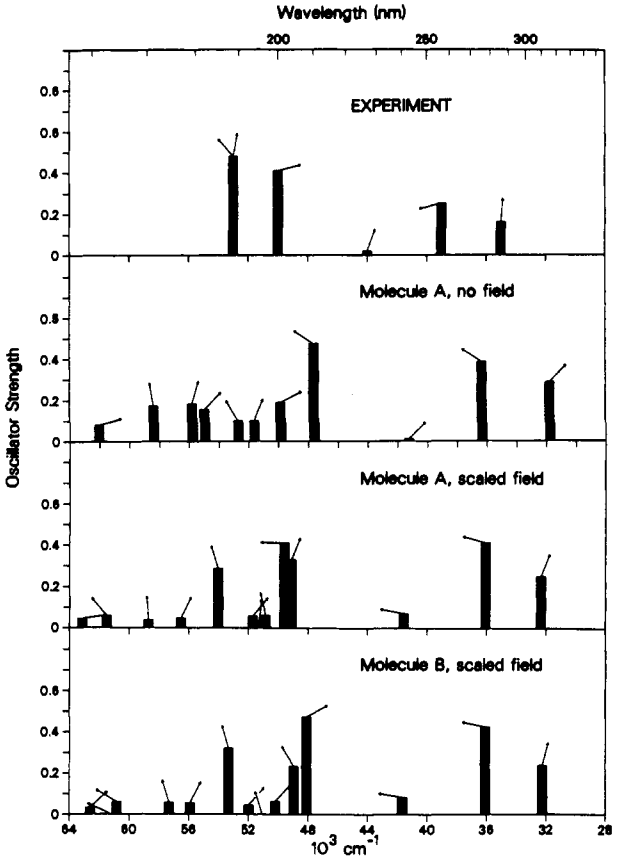

Figure 6. Comparison of experimental transition parameters for 9-ethylguanine crystals[2] with theoretical values obtained for the isolated molecule (no field) and for molecules A and B in the crystal. For numerical values, see Table III.

in unscaled calculations on molecule A by $n\pi^*$–$\pi\pi^*$ mixing, which makes the second "$\pi\pi^*$ transition" very weak. However, this is an artifact of our arbitrary distinction between $n\pi^*$ and $\pi\pi^*$ transitions. This excited state has largely $n\pi^*$ parentage but, because of its proximity in energy to the second $\pi\pi^*$ excited state, acquires significant intensity and is polarized only 8° out of plane. If we combine the intensities of $\pi\pi^*$ transitions 2 and 3 for molecule A, we obtain an oscillator strength of 0.39, which is somewhat greater than that of transition 2 in the isolated molecule.)

Examination of the CI coefficients for the two lowest $\pi\pi^*$ excited states reveals that the HOMO → LUMO and HOMO → LUMO + 1 transitions are the dominant contributors (ca. 95%) in the calculations with and without the crystal field. In the presence of the field, the HOMO → LUMO configuration is not as dominant in the first excited state as it is in the absence of the field (65% vs 90%). Correspondingly, the HOMO → LUMO + 1 configuration is less dominant in the second excited state in the presence of the field (61% vs 87%).

The crystal field has a significant effect on the shape of the MOs themselves. These are shown in Figure 7. The HOMO is altered very little by the crystal field, but the LUMO and LUMO + 1 are changed substantially. The LUMO + 1 in the absence of the field resembles the LUMO in the presence of the field. The field-free LUMO resembles the LUMO + 1 in the presence of the field to a lesser extent, but the nodal patterns correspond. Thus, the major effect of the field is on the virtual MOs, and the LUMO and LUMO + 1 are, to a first approximation, interchanged by application of the crystal field.

The third predicted $\pi\pi^*$ transition corresponds to a weak transition for which no polarization direction was determined.[2] The effect of the crystal field is to enhance the intensity of this transition relative to that in the isolated molecule. The polarization is also dramatically altered, approaching that of the second $\pi\pi^*$ transition. The increase in intensity and shift in polarization

Table V. Comparison of Models[a] for Observed Absorption Bands

band	expt λ	expt f[b]	expt θ[c]	model 1 λ[d]	model 1 f[d]	model 1 θ[e]	model 2 λ[d]	model 2 f[d]	model 2 θ[e]	model 3 λ[d]	model 3 f[d]	model 3 θ[e]
						Scaled Calculations						
I	273	0.16	**−4**, +35	310	0.24	−18, +53	310	0.24	−18, +53	310	0.24	−18, +53
II	249	0.25	−75	277	0.42	+76, −41	277	0.42	+76, −41	277	0.42	+76, −41
M	227			240	0.08	+79, −44	240	0.08	+79, −44	240	0.08	+79, −44
III	204	0.42	−71, −79	205[f]	0.44	−86, −59	205[i]	0.73	−37, +72	205[f]	0.44	−86, −59
IV	189	0.50	**−9**, +41	203[g]	0.28	−11, +46	187[h]	0.30	+16, +19	195[j]	0.58	−2, +38
				187[h]	0.30	+16, +19						
						Unscaled Calculations						
I	273	0.16	**−4**, 35	312	0.23	−10, +45	312	0.23	−10, +45	312	0.23	−10, +45
II	249	0.25	−75	280[k]	0.39	+81, −45	280[k]	0.39	+81, −45	280[k]	0.39	+81, −45
M	227			239	0.13	+88, −52	239	0.13	+88, −52	239	0.13	+88, −52
III	204	0.42	−71, −79	210[g]	0.49	−42, +77	207[n]	0.76	−37, +72	210[g]	0.49	−42, +77
IV	189	0.50	**−9**, +41	203[l]	0.27	−28, +64	187[m]	0.45	−2, +37	194[o]	0.70	−15, +50
				187[m]	0.45	−2, +37						

[a] See text and footnotes *f–o* for description of the models, which differ only in the far ultraviolet. [b] Two possible values for the oscillator strength in the crystal are given by Clark[2] for several transitions, corresponding to different choices of transition moment directions. These values differ by only a few percent and have been averaged in this table. [c] Where two values are given, both are consistent with experiment.[2] The value in boldface is that preferred by Clark.[2] Clark's estimate of the uncertainty in these values is ±4°. [d] For description of how average wavelengths and oscillator strengths were calculated, see Methods. [e] For description of how the average transition moment direction was calculated, see Methods. The two possible values are both given. [f] $\pi\pi^*$ transition 4 of molecule A + 5 of molecule B. [g] $\pi\pi^*$ transition 5 of molecule A and 4 of molecule B. [h] $\pi\pi^*$ transition 9 of molecules A and B. [i] $\pi\pi^*$ transitions 4 and 5 of molecules A and B. [j] $\pi\pi^*$ transitions 5 and 9 of molecule A + transitions 4 and 9 of molecule B. [k] $\pi\pi^*$ transitions 2 and 3 of molecule A + transition 2 of molecule B. [l] $\pi\pi^*$ transitions 6 and 7 of molecule A + transitions 5 and 6 of molecule B. [m] $\pi\pi^*$ transitions 8–11 of molecule A + transitions 7–11 of molecule B. [n] $\pi\pi^*$ transitions 5–7 of molecule A + transitions 4–6 of molecule B. [o] $\pi\pi^*$ transitions 6–10 of molecule A + transitions 5–9 of molecule B.

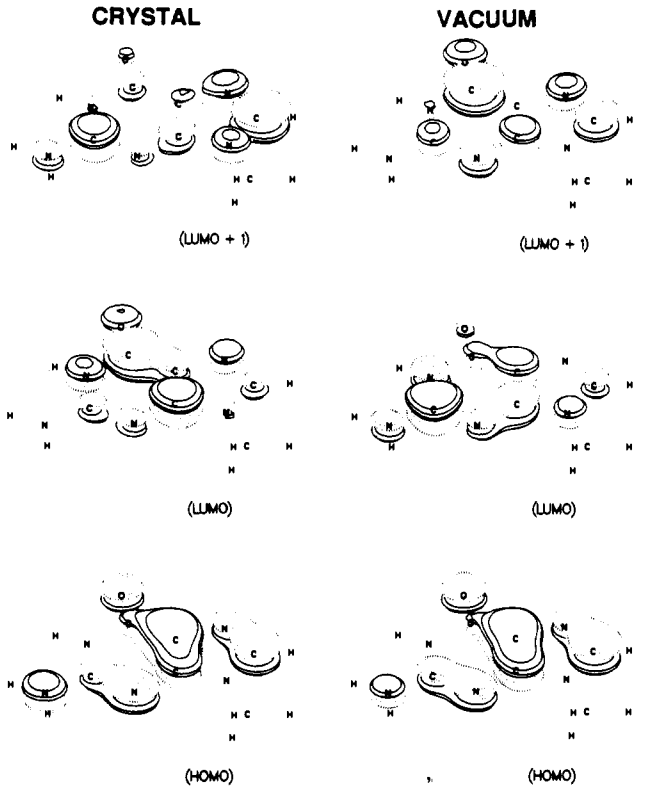

Figure 7. Representation of the highest occupied molecular orbital (HOMO) of 9-methylguanine and the lowest and next lowest unoccupied molecular orbitals (LUMO and LUMO + 1, respectively). These are shown for calculations on the molecule in the scaled crystal field and for the isolated molecule. Positive regions of the wave function are represented by solid contours and negative regions by dotted contours.

direction are due to mixing of the intrinsically weak third transition in the isolated molecule with other $\pi\pi^*$ transitions, primarily the second $\pi\pi^*$ transition. Although no estimate of the oscillator strength of this band (the M band) was given by Clark, he gave a value of 0.01–0.03 for a corresponding band in protonated guanine. Both calculations with crystal fields exceed this intensity, but the scaled calculations give a smaller intensity. The higher energy region of the spectrum presents serious difficulties for both theory and experiment. Clark[2] reported two strong absorption bands in the 170–210-nm region with polarizations shown in Figure 1 and Table V. Calculations on the isolated molecules predict only one band in this region with an oscillator strength greater than 0.2 (Table III). This band is at 210 nm, and its polarization (ca. +55°) is very different from Clark's observed band III (ca. −75°). The calculations on the isolated molecule predict five additional bands between 202 and 179 nm, with oscillator strengths ranging from 0.1 to 0.2.

The predicted spectrum is simplified upon inclusion of the crystal field. This is especially true for the scaled field calculations, for which only three transitions with significant intensity are predicted for wavelengths down to 160 nm, with all other transitions having $f \leq 0.06$. Table V presents several possible correlations of the strong $\pi\pi^*$ transitions calculated by using a scaled field with the experimentally observed bands.[2] The theoretical band parameters reported in Table V represent averages over both molecules A and B and one or more transitions.

For the scaled calculations, model 1 correlates the two nearly degenerate $\pi\pi^*$ transitions predicted to occur just above 200 nm with bands III and IV of Clark.[2] It can be seen from Table V that although this model gives reasonable polarization directions for both bands, the relative intensities predicted for bands III and IV are not satisfactory, nor is the position of band IV. In addition, the third predicted band does not correlate with any of the well-characterized observed bands.

Model 2 correlates the two nearly degenerate transitions above 200 nm with Clark's[2] band III and the moderately strong transition at 187 nm with band IV. This model gives much less satisfactory transition moment directions and even poorer agreement with the observed relative oscillator strengths.

Model 3 combines the weaker of the two transitions predicted to lie above 200 nm with that predicted for 187 nm. This model gives satisfactory agreement with the observed parameters for bands III and IV, although it implies that the calculations are underestimating the energy of transition 4 in molecule A and transition 5 in molecule B.

For the unscaled calculations, models 1–3 are constructed along the lines of those for the scaled calculations, but more transitions are included because the oscillator strength is distributed more widely. In general, the agreement with experiment for each model is less satisfactory for the unscaled calculations than for those which were scaled.

The predicted parameters for the $n\pi^*$ transitions of 9-ethylguanine crystals are given in Table IV. In accord with expec-

tations, the crystal field blue shifts the $n\pi^*$ transitions. The longest wavelength $n\pi^*$ transition is blue-shifted by ca. 30 nm in the scaled calculations and by 40 nm in the unscaled. (Note that in the unscaled calculations on molecule A the lowest energy $n\pi^*$ transition has been obscured by mixing with the $\pi\pi^*$ manifold and has been classified as a $\pi\pi^*$ transition by our criterion.) In the gas-phase calculations, the lowest excited state is $n\pi^*$ but, in the crystal, the first $n\pi^*$ excited state falls between the two lowest energy $\pi\pi^*$ excited states.

With respect to intensity, in the scaled crystal field calculations, only the $n\pi^*$ band predicted for ca. 215 nm has a significant intensity in absorption, with an oscillator strength of ca. 0.03. The unscaled calculations also indicate a relatively strong $n\pi^*$ band at slightly shorter wavelength (ca. 210 nm).

The crystal field extensively mixes $n\pi^*$ and $\pi\pi^*$ transitions, as reflected in the deviations of the angle ϕ between the transition moment and the molecular plane from the 90° characteristic of pure $n\pi^*$ transitions. The extent of this mixing has important implications for the circular dichroism (CD) spectrum of nucleic acids. The CD intensity of a transition depends on the scalar product of the electric and magnetic dipole transition moments.[32] Mixing of $n\pi^*$ and $\pi\pi^*$ transitions can lead to substantial CD intensity because $n\pi^*$ transitions generally have strong in-plane magnetic dipole transition moments, while $\pi\pi^*$ transitions have strong in-plane electric dipole transition moments. Such $n\pi^*$–$\pi\pi^*$ mixing due to local electrostatic fields (the one-electron contribution[33]) has long been recognized as essential for accounting for peptide CD spectra[34,35] but, with a few exceptions,[36-38] has been neglected in theoretical calculations on nucleic acids. The present results indicate that these contributions may be substantial and need to be considered.

Experimentally, there is a dearth of information on $n\pi^*$ transitions in the nucleic acid bases, with data on guanine being especially sparse. Clark[2] suggested that a weak feature observed near 300 nm in the reflection spectrum of 9-ethylguanine crystals, polarized normal to the molecular planes, may be an $n\pi^*$ transition. However, he noted that this feature could also be due to a shifted $0 \rightarrow 0$ component of the first $\pi\pi^*$ transition. If this feature is an $n\pi^*$ transition, our theoretical prediction that the first $n\pi^*$ transition in 9-ethylguanine crystals falls between the first and second $\pi\pi^*$ transitions is incorrect.

In summary, we have shown that local electrostatic fields in 9-ethylguanine crystals have a significant effect upon the electronic spectral parameters. In particular, these local fields alter the transition moment directions of the $\pi\pi^*$ transitions and mix $n\pi^*$ with $\pi\pi^*$ transitions. It is necessary to consider these interactions in interpreting the absorption and circular dichroism spectra of crystals of the bases and of oligo- and polynucleotides.

Acknowledgment. This work was supported by NIH Grants GM31824 to P.R.C. and GM22994 to R.W.W. and by a Fogarty Senior International Fellowship to R.W.W. We thank Drs. Andrey Volosov and N. Sreerama for helpful discussions and comments.

Registry No. 9-Ethylguanine, 879-08-3.

(32) Rosenfeld, L. *Z. Phys.* **1928**, *52*, 161.
(33) Condon, E. U.; Altar, W.; Eyring, H. *J. Chem. Phys.* **1937**, *5*, 753.
(34) Schellman, J. A.; Oriel, P. *J. Chem. Phys.* **1962**, *37*, 2114.
(35) Woody, R. W.; Tinoco, I., Jr. *J. Chem. Phys.* **1967**, *46*, 4927.
(36) Bush, C. A.; Brahms, J. *J. Chem. Phys.* **1967**, *46*, 79.
(37) Bush, C. A. *J. Chem. Phys.* **1970**, *53*, 3522.
(38) Studdert, D. S.; Davis, R. C. *Biopolymers* **1974**, *13*, 1391.

Influence of Molecular Dipole Interactions on Solid-State Organization

James K. Whitesell,* Raymond E. Davis,* Lisa L. Saunders, Robb J. Wilson, and John P. Feagins

Contribution from the Department of Chemistry, The University of Texas at Austin, Austin, Texas 78712. *Received October 10, 1990*

Abstract: A statistical analysis of molecular dipole moments within three space groups ($P1$, $P\bar{1}$, and $P2_1$) was carried out. The magnitude of the molecular dipole moment does not vary significantly between centrosymmetric ($P\bar{1}$) and noncentrosymmetric ($P1$ and $P2_1$) space groups and does not correlate with relative molecular orientations within the $P2_1$ space group. Thus, the high preference for organic molecules to crystallize in one of the centrosymmetric arrangements cannot be attributed to dipole–dipole interactions.

The detailed study of regular and semiregular molecular arrays such as single crystals and liquid crystals has moved into prominence in recent years as the potential for practical applications of such systems has fluorished. Because of our interest in developing new methods for manipulating multimolecular arrays for practical applications, we became aware of the common idea that large molecular dipole moments are an important factor leading to centrosymmetry in organic crystals.[1] This notion appears to be held by many researchers in the area of nonlinear optics, as evidenced by statements such as the following: "It is clear that as the molecular ground-state dipoles become larger, the electrostatic interraction between adjacent molecules increases and the net molecular dipole alignment required to achieve the maximum crystal anisotropy becomes more energetically unfavorable";[2] and "...it is hypothesized that a correlation between the dipolar and conjugation characteristics of nonlinearly enhanced molecules and the common occurrence of antiparallel alignments exists."[3] Because the design of new methods for molecular

(1) Centrosymmetric arrangements are statistically favored in organic crystals. Of the entries in the Cambridge Structural Database (January 1990 release), 67% are in one of the centrosymmetric space groups. However, crystal structures based on single enantiomers (a substantial fraction of the collection) *cannot* be centrosymmetric. Thus, the value of 67% represents a *lower limit* for the bias toward centrosymmetry; the figure is surely far higher for molecules that could adopt either centrosymmetric or noncentrosymmetric arrangements.

(2) Nicoud, J. F.; Twieg, R. J. In *Non-Linear Optical Properties of Organic Molecules and Crystals*; Chemla, D. S., Zyss, J., Eds.; Academic Press, Inc.: New York, 1987; Vol. 1, p 253.
(3) Meredith, G. R. In *Non-Linear Optical Properties of Organic and Polymeric Materials*; Williams, D. J., Ed.; ACS Symp. Ser. 233; American Chemical Society: Washington, DC, 1983; p 29.

0002-7863/91/1513-3267$02.50/0